Neuro-Oncology

25(1), 185–198, 2023 | https://doi.org/10.1093/neuonc/noac147 | Advance Access date 31 May 2022

Activation of Hedgehog signaling by the oncogenic RELA fusion reveals a primary cilia-dependent vulnerability in supratentorial ependymoma

Taciani de Almeida Magalhães, Gustavo Alencastro Veiga Cruzeiro, Graziella Ribeiro de Sousa, Bernhard Englinger, Luis Fernando Peinado Nagano, Mathew Ancliffe, Keteryne Rodrigues da Silva, Li Jiang, Johannes Gojo, Yulu Cherry Liu, Brooke Carline, Mani Kuchibhotla, Fabiano Pinto Saggioro, Suely Kazue Nagahashi Marie, Sueli Mieko Oba-Shinjo, José Andres Yunes, Rosane Gomes de Paula Queiroz, Carlos Alberto Scrideli, Raelene Endersby, Mariella G. Filbin, Kleiton Silva Borges, Adrian Salic, Luiz Gonzaga Tone, and Elvis Terci Valera

Department of Genetics, Ribeirão Preto Medical School, University of São Paulo, Ribeirão Preto, São Paulo, Brazil (T.A.M., G.R.S., L.F.N., K.R.S., L.G.T.); Department of Cell Biology, Harvard Medical School, Boston, Massachusetts, USA (T.A.M., Y.C.L., A.S.); Department of Pediatrics, Ribeirão Preto Medical School, University of São Paulo, Ribeirão Preto, São Paulo, Brazil (G.A.V.C., R.G.P.Q., C.A.S., K.S.B., L.G.T., E.T.V.); Department of Pediatric Oncology, Dana-Farber Boston Children's Cancer and Blood Disorders Center, Boston, Massachusetts, USA (G.A.V.C., B.E., L.J., J.G., M.G.F.); Broad Institute of Harvard and MIT, Cambridge, Massachusetts, USA (G.A.V.C., B.E., L.J., M.G.F.); Department of Urology, Comprehensive Cancer Center, Medical University of Vienna, Vienna, Austria (B.E.); Brain Tumour Research Program, Telethon Kids Institute and the University of Western Australia, Nedlands, Western Australia, Australia (M.A., K.R.S., B.C., M.K., R.E.); Department of Pediatrics and Adolescent Medicine, Comprehensive Center for Pediatrics, Medical University of Vienna, Vienna, Austria (J.G.); Department of Pathology, Ribeirão Preto Medical School, University of São Paulo, Ribeirão Preto, São Paulo, Brazil (F.P.S.); Cellular and Molecular Biology Laboratory, Department of Neurology, Faculdade de Medicina (FMUSP), University of São Paulo, São Paulo, Brazil (S.K.N.M., S.M.O.); Molecular Biology Laboratory, Boldrini Children's Center, Campinas, São Paulo, Brazil (J.A.Y.); Division of Endocrinology, Boston Children's Hospital, Boston, Massachusetts, USA (K.S.B.)

Corresponding Authors: Taciani de Almeida Magalhaes, PhD, Department of Cell Biology, Harvard Medical School, Boston, MA 02115, USA (taciani_magalhaes@hms.harvard.edu); Elvis Terci Valera, MD, PhD, Department of Pediatrics, Ribeirão Preto Medical School, University of São Paulo, 3900 Bandeirantes Avenue, Ribeirão Preto, SP 14049-900, Brazil (etvalera@hcrp.usp.br).

Abstract

Background. Supratentorial RELA fusion (ST-RELA) ependymomas (EPNs) are resistant tumors without an approved chemotherapeutic treatment. Unfortunately, the molecular mechanisms that lead to chemoresistance traits of ST-RELA remain elusive. The aim of this study was to assess RELA fusion-dependent signaling modules, specifically the role of the Hedgehog (Hh) pathway as a novel targetable vulnerability in ST-RELA.

Methods. Gene expression was analyzed in EPN from patient cohorts, by microarray, RNA-seq, qRT-PCR, and scRNA-seq. Inhibitors against Smoothened (SMO) (Sonidegib) and Aurora kinase A (AURKA) (Alisertib) were evaluated. Protein expression, primary cilia formation, and drug effects were assessed by immunoblot, immunofluorescence, and immunohistochemistry.

Results. Hh components were selectively overexpressed in EPNs induced by the RELA fusion. Single-cell analysis showed that the Hh signature was primarily confined to undifferentiated, stem-like cell subpopulations. Sonidegib exhibited potent growth-inhibitory effects on ST-RELA cells, suggesting a key role in active Hh signaling; importantly, the effect of Sonidegib was reversed by primary cilia loss. We, thus, tested the effect of AURKA inhibition by Alisertib, to induce cilia stabilization/reassembly. Strikingly, Alisertib rescued ciliogenesis and synergized with Sonidegib in killing ST-RELA cells. Using a xenograft model, we show that cilia loss is a mechanism for acquiring resistance to the inhibitory effect of Sonidegib. However, Alisertib fails to rescue cilia and highlights the need for other strategies to promote cilia reassembly, for treating ST-RELA tumors.

Conclusion. Our study reveals a crucial role for the Hh pathway in ST-RELA tumor growth, and suggests that rescue of primary cilia represents a vulnerability of the ST-RELA EPNs.

Key Points

- Hh pathway is hyperactivated in ST-RELA tumors and is induced by the RELA fusion.
- ST-RELA cells lose primary cilia as an adaptive escape mechanism to Hh inhibition.
- Hh signaling is a primary cilia-dependent therapeutic vulnerability of ST-RELA tumors.

Importance of the Study

The absence of novel therapeutic targets for ST-RELA tumors is a major current challenge. We discovered a specific gene expression signature of the Hh pathway in ST-RELA, specifically enriched in undifferentiated and actively dividing cell populations, which we show is directly induced by the RELA fusion and is dependent on Hh ligand. We also reveal that loss of cilia in ST-RELA cells is an unappreciated mechanism for escape from Hh inhibition, both in vitro and in vivo. Consistent with this idea, we find a striking pharmacological synergy between primary cilia stabilization via AURKA inhibition by Alisertib and Hh pathway inhibition by Sonidegib in cultured tumor cells. However, Alisertib fails to induce cilia reassembly in vivo, which limits the efficacy of the drug combination above. These findings reveal the critical need to rescue primary cilia as a strategy to promote vulnerability to Hh inhibition of highly aggressive ST-RELA tumors.

Ependymoma (EPN) is the third most common pediatric malignancy of the central nervous system (CNS). EPN is a heterogeneous disease, with some tumors exhibiting an aggressive clinical course, while others following a more favorable course.[1] The molecular classification of EPN subgroups comprises nine molecular entities, with unique genetic, epigenetic, and clinical features. According to this classification, EPNs can be supratentorial (ST) (ST-subependymoma, ST-YAP1, ST-RELA), posterior fossa (PF) (PF-subependymoma, PF-A, PF-B), and spinal (SP) (SP-subependymoma, SP-myxopapillary, SP-EPN).[2–5] The ST-RELA subgroup is characterized by oncogenic fusions, most frequently, between exon 2 (type 1) or exon 3 (type 2) of *C11orf95* (also known as *ZFTA*), and exon 2 of *RELA* (ZFTA-RELA).[6,7] This subtype accounts for approximately 72% of all childhood ST-EPNs and is resistant to both chemotherapy and targeted small molecule inhibitors.[8–10] Several retrospective studies point to a low overall survival among ST-EPNs patients (as low as 30% in 5 years).[9,10]

Although the chemoresistance and aggressiveness of ST-RELA tumors are related to proliferative and stemness signatures resulting from aberrant developmental processes, their molecular mechanisms have not yet been elucidated.[10,11] The Hedgehog (Hh) pathway is a critical regulator of CNS development, including morphogenesis of radial glial cells, the likely stem cells that give rise to EPNs.[12–14] Hh activation is initiated by the binding of Hh ligands, Sonic (SHH), Desert (DHH), or Indian (IHH), to the tumor suppressor membrane protein, Patched1 (PTCH1), a negative regulator of Hh signaling, causing its inhibition and removal from the primary cilia.[13,15] Consequently, the oncoprotein Smoothened (SMO) becomes active and accumulates in cilia, leading to activation of the GLI zinc finger proteins, by removing the inhibition exerted by the suppressor of fused (SUFU) protein.[13,15] Once activated, GLI proteins translocate to the nucleus and turn on the transcription of Hh target genes, which orchestrate cellular growth, survival, and stem cell maintenance.[13,15] Aberrant expression or mutations in Hh pathway components might promote formation of CNS tumors and their resistance to therapy.[13,16]

In vertebrates, Hh signaling relies on primary cilia, microtubule-based organelles that extend from the surface of most cells.[17] Thus, primary cilia can mediate Hh-dependent tumor formation and aggressiveness.[18–20] Consistent with this idea, preclinical studies have highlighted the presence of primary cilia as a therapeutic marker that correlates with the efficacy of SMO inhibitors.[18,21,22] Conversely, cilia loss contributes to reduced sensitivity of CNS tumors to SMO antagonists.[17] Despite the critical function of cilia-dependent Hh signaling in CNS tumor aggressiveness, the role of the Hh pathway in ST-RELA EPNs has not been explored.

Here, we investigate the involvement of the Hh pathway in ST-RELA tumors, and its relevance as a potential therapeutic target. We find that components of the Hh pathway are selectively overexpressed in ST-RELA, induced by the RELA fusion. However, ST-RELA cells show a limited response to the Hh inhibitor, Sonidegib, due to a therapeutic escape mechanism caused by cilia loss. We demonstrate that the Aurora kinase A (AURKA) inhibitor, Alisertib, induces primary cilia reassembly in ST-RELA cells, which, in turn, greatly enhances their vulnerability to Sonidegib. Our xenograft studies confirm that cilia loss impairs the effect of Sonidegib. Surprisingly, however, Alisertib fails to rescue

primary cilia assembly in vivo, thus affecting the efficacy of its combination with Sonidegib. Together, our findings suggest that undifferentiated and cycling ST-RELA tumor cell niches are specifically vulnerable to inhibition of cilia-dependent Hh signaling, and point to the critical importance of pharmacological rescue of primary cilia as a strategy to counteract resistance of ST-RELA tumor to Hh blockade.

Materials and Methods

Patients and Samples

A total of 34 pediatric (25 primary and 9 relapse) EPN patients diagnosed and treated between 1999 and 2017, were molecularly classified into ST-RELA (n = 9), ST-YAP1 (n = 3), and PF-A (n = 22) groups.[23] The clinical and molecular features of each patient are shown in Supplementary Table 1. This research was performed under the approval of the HC/FMRP-USP Research Ethics Committee (CAAE n°37206114.1.0000.5440) and National Research Ethics Commission (CONEP/B-028) (CAAE n° 25574714.9.0000.5376). Detailed information is found in the Supplementary Material.

Cell Culture

The following cell lines were used in this study: HEK-293T cells; mouse embryonic fibroblasts (MEFs and NIH-3T3); ST-RELA cells: BXD-1425EPN (kindly provided by Dr Xiao-Nan Li[24]), DKFZ-EP1NS (kindly provided by Dr Till Milde[25]); and the PF-A cell line, MAF928 (kindly provided by Dr Nicholas K Foreman[26]). These cells are described in the Supplementary Material. The presence of the RELA fusion in ST-RELA cells was confirmed by immunoblot (Supplementary Figure 1A).

Gene Expression Analysis

EPN samples for which high-quality RNA was available (n = 10) were analyzed on the TruSeq Stranded Total RNA Human (Illumina) (GSE181162). Gene expression was downloaded from Gene Expression Omnibus (GEO) and analyzed using microarray (GSE64415)[2] and scRNA-seq (GSE141460)[11] dataset of EPN patients. Detailed information is provided in the Supplementary Material.

Reagents and Materials

The lentiviral vector pCDH-MSCV-EF1-GFP was used to drive the expression of the type I fusion ($RELA^{FUS1}$), $RELA^{WT}$, and ZFTA (kindly provided by Dr Richard Gilbertson[10,27]). Sequences encoding gRNAs directed against the genes for human intraflagellar transport protein 88 (*IFT88*), *SMO*, or *GLI2* were subcloned into the hSpCas9-2A-Puro plasmid (PX459) (#62988, Addgene). The resulting plasmids were transfected using Lipofectamine 3000 Reagent (Invitrogen), to generate clonal cells depleted of the indicated genes.[28] Detailed reagent information is provided in the Supplementary Material.

Quantitative Reverse Transcription PCR, Western Blot, Immunofluorescence, and DHH Release Assays

Quantitative reverse transcription PCR (qRT-PCR), Western blot (WB), immunofluorescence (IF), and DHH release assay were performed as described.[9,29] TaqMan probes, primers, and antibodies used for WB and IF are listed in Supplementary Tables 2–5. Detailed information is found in the Supplementary Material.

Cell Proliferation, Colony-Forming, Cell Death, Cell Cycle, and Drug Synergy Assays

In vitro assays were performed as described.[9] Detailed information is found in the Supplementary Material.

Immunohistochemistry

Immunohistochemistry (IHC) on formalin-fixed paraffin-embedded (FFPE) mouse brain tissue sections (5 µm) and human tissue sections (4 µm) was performed as described in the Supplementary Material. Antibodies used for IHC are listed in Supplementary Table 6.

In Vivo Studies

Animal experiments were approved by the Animal Ethics Committee of the Telethon Kids Institute and were performed in accordance with Australia's Code for the Care and Use of Animals for Scientific Purposes. The orthotopic patient-derived xenograft (O-PDX) using IC-1425EPN cells[24] was performed as described in the Supplementary Material.

Statistics

Data analysis was carried out using SPSS 22.0 or GraphPad Prism 9.0. Analysis included Student's *t* test, Wilcoxon rank test, or one-way ANOVA test, followed by Bonferroni test. Differences in gene expression are represented by fold-change (FC). Pearson was utilized for correlations. Molecular and functional assays are reported as mean ± SE of three independent experiments, performed in duplicate or triplicate. qRT-PCR, WB, and IF experiments were independently replicated at least twice. $P < .05$ was statistically significant.

Results

Hh Pathway Components Are Selectively Overexpressed in ST-RELA Tumors

To assess the transcriptional signature of the Hh pathway (KEGG gene set hsa_04340) in EPN subtypes, we performed unsupervised hierarchical cluster analysis using the EPN microarray dataset (GSE64415),[2] which contains a cohort composed of ST-RELA (n = 49), PF-A (n = 72), ST-YAP1 (n = 11), and PF-B (n = 39) patients. Interestingly,

we identified specific overexpression of a set of core Hh pathway components (*DHH*, *GLI2*, and *GLI3*[18]) and target genes (*CSNK1G2*, *SMURF2*, *MGRN1*, *CCND1*, *KIF7*, and *PRKACA*[18]) in ST-RELA, but not in other subgroups (PF-A, ST-YAP1, and PF-B) (Figure 1A). To validate our in silico analysis, we also assessed the transcriptional signature of the NF-κB pathway, a molecular hallmark of ST-RELA tumors.[2,27] As expected, we found a specific NF-κB signature in ST-RELA samples (Supplementary Figure 1B), suggesting that our approach is effective in validating pathway signatures across molecular subgroups. Additionally, we performed KEGG pathway enrichment analysis using the differentially expressed genes of ST-RELA over all other subgroups from the microarray dataset.[2]This analysis indicated that basal cell carcinoma is the top-ranked pathway for ST-RELA tumors. Importantly, basal cell carcinoma is driven by aberrant Hh signaling[30] and is annotated mainly by WNT and Hh genes, such as *GLI2*, *KIF7*, *DDB2*, and *BAX* (Supplementary Figure 1C), further supporting our exploration of the Hh pathway in ST-RELA tumors.

We next validated the expression of Hh components in a second independent cohort of EPNs, with 34 patients previously subgrouped as ST-YAP1 (n = 3), ST-RELA (n = 9), and PF-A (n = 22),[23] as well as in ST-RELA in vitro models (BXD-1425 and EP1NS cells). We first generated the Hh transcriptomic signature for all samples for which sufficiently high-quality RNA was available (n = 10). Supervised hierarchical cluster analysis also revealed specific overexpression of *DHH*, *GLI2*, and the Hh target genes *CSNK1G2*, *CCND1*, *KIF7*, *PRKACA*, *MGRN1*, and *SMURF2*[18] in ST-RELA over other subgroups (Supplementary Figure 2A). Using qRT-PCR and non-neoplastic brain cDNA as calibrator, we found a similar profile characterized by high expression of *DHH*, *SMO*, *GLI1*, *GLI2*, and *GLI3* in ST-RELA samples and cell lines compared to other EPN subgroups. Additionally, *SHH*, *IHH*, *PTCH1*, and *SUFU* were downregulated in our ST-RELA samples and cell lines (Supplementary Figure 2B–J), as observed in the discovery cohorts.

Finally, to validate the expression of Hh ligands at the protein level in patient tissue, we performed IHC staining for DHH, SHH, and IHH in FFPE specimens. Although the number of FFPE samples was limited, we observed that ST-RELA tumors showed higher scores for DHH staining compared to ST-YAP1 tumors, while SHH and IHH staining revealed no differences between EPN subgroups (Figure 1B). Together, these results indicate that key Hh pathway components are differentially overexpressed in ST-RELA subgroup, suggesting that Hh signaling might play an important role.

Single-Cell Analysis Reveals that Hh Pathway Components Are Enriched in Undifferentiated and Cycling ST-RELA Cell Populations

We next used a scRNA-seq dataset (GSE141460) of EPN tumors[11] to confirm our findings from bulk tumor microarray data. Using the same subset of Hh genes, we scored relative expression for each cell[32] and determined that Hh components are significantly enriched in ST-RELA tumors over other subgroups (Figure 1C). On a single-gene level, *DHH*, *SMO*, and *GLI2* were significantly upregulated in ST-RELA compared to other subgroups (Figure 1D).

To dissect the Hh signature and its potential role in ST-RELA in more detail, we explored Hh pathway enrichment in heterogeneous ST-RELA cell types.[11] Interestingly, we found that the Hh program is enriched in primitive, actively dividing cell types that likely represent tumor stem cell compartments: ST-RELA-Variable, ST-Neuronal-Precursor-like, and ST-Radial-Glia-like. In contrast, the Hh gene set scored low in metaprograms that characterize favorable prognosis (eg, ST-Ependymal-like)[11] (Figure 2A). On a single-gene level, *DHH*, *SMO*, and *GLI2* were enriched in cycling and undifferentiated subpopulations (Figure 2B–D). Conversely, *GLI3* was expressed both in undifferentiated and differentiated cells, possibly because GLI3 functions as both positive and negative Hh regulator, depending on its proteolytic state[19] (Figure 2E). Taken together, our single-cell data indicate that the Hh program is enriched in proliferative and stemness-associated cell subpopulations, substantiating the hypothesis that Hh signaling plays a key role in these cells. Additionally, these data further support the use of Hh inhibitors, to specifically target cycling and stem-like ST-RELA compartments.

Ligand-dependent Hh Signaling Is Induced by the Oncogenic RELA Fusion

Since Hh driver mutations are not found in ST-RELA tumors,[2,33] we hypothesized that the observed Hh signature is induced by the oncogenic ZFTA-RELA transcription factor.[27] Analysis of the GSE64415 dataset[2] revealed a positive correlation between expression of *RELA* and that of *DHH* ($R = 0.6075$, $P = .0004$) and *GLI2* ($R = 0.6628$, $P < .0001$) (Supplementary Figure 3A). To test whether ZFTA-RELA drives Hh gene expression, we stably transduced NIH-3T3 cells with the $RELA^{FUS1}$ fusion (Supplementary Figure 3B and C). We used NIH-3T3 cells because they display robust primary cilia and mount a strong response to Hh ligands.[34] Interestingly, $RELA^{FUS1}$ expression caused a significant increase in SMO and GLI accumulation in primary cilia, while expression of ZFTA or $RELA^{WT}$ alone had no effect (Figure 3A); this result shows that $RELA^{FUS1}$ leads to activation of the Hh pathway. We also examined the effect of $RELA^{FUS1}$ expression in HEK-293T cells and found high expression of *DHH*, *SMO*, *GLI2*, and *GLI3* compared to control cells expressing ZFTA or $RELA^{WT}$ (Figure 3B). Notably, we also observed high expression of *DHH*, *SMO*, *GLI1*, and *GLI3* in HEK-293T $RELA^{WT}$ cells compared to control or ZFTA, which is consistent with previous findings showing that RELA may activate Hh signaling through Hh ligand induction.[35] Moreover, DHH protein levels were increased in both NIH-3T3 and HEK-293T cells by $RELA^{FUS1}$, and at lower levels in HEK-293T by $RELA^{WT}$ (Supplementary Figure 3D). Finally, we asked whether increased DHH levels lead to accumulation of full-length (FL) GLI proteins, another hallmark of Hh activation.[18] As shown in Figure 3C, subcellular fractionation of NIH-3T3 $RELA^{FUS1}$ and HEK-293T $RELA^{WT}$ and $RELA^{FUS1}$ cells revealed increased levels of GLI2/3FL in the nucleus, together with reduction of the GLI repressor form (GLI3R). Taken together, our findings indicate that the

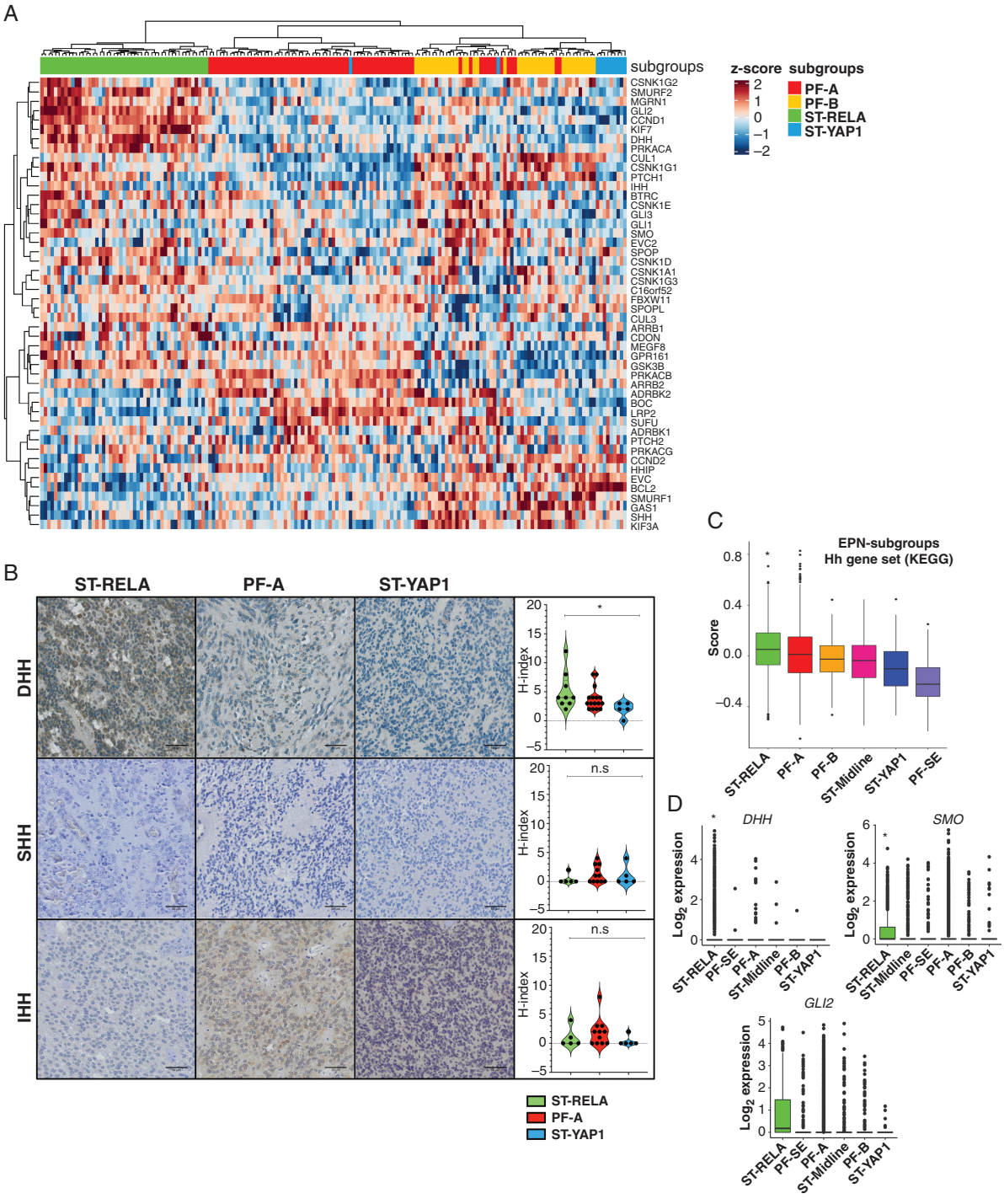

Fig. 1 Hh pathway components are specifically overexpressed in ST-RELA tumors. (A) Heatmap representation of an unsupervised Hh signature across EPN subgroups (GSE64415)[2] based on the KEGG_Hh pathway_hsa_04340. (B) Representative immunohistochemistry images and H-score[31] of DHH, SHH, and IHH staining in ST-RELA, PF-A, and ST-YAP1 samples (scale bar = 50 µm). *$P < .05$, one-way ANOVA followed by Bonferroni test (scale bar = 50 µm). (C) Hh gene set score (KEGG_Hh pathway-hsa_04340); *$P < .05$, Wilcoxon rank test; and (D) log-transformed *DHH*, *SMO*, and *GLI2* expression across EPN subgroups (GSE141460).[11] *$P < 0.05$, one-way ANOVA followed by Bonferroni test.

RELA fusion promotes Hh pathway activation, by inducing DHH ligand expression.

To confirm this hypothesis, we next investigated whether DHH is secreted by ST-RELA cells. All Hh ligands are strongly membrane-associated, due to modification with both cholesterol and palmitate, and require a secreted SCUBE family protein, such as SCUBE2, for release from cells.[29] Addition of purified SCUBE2 to BXD-1425

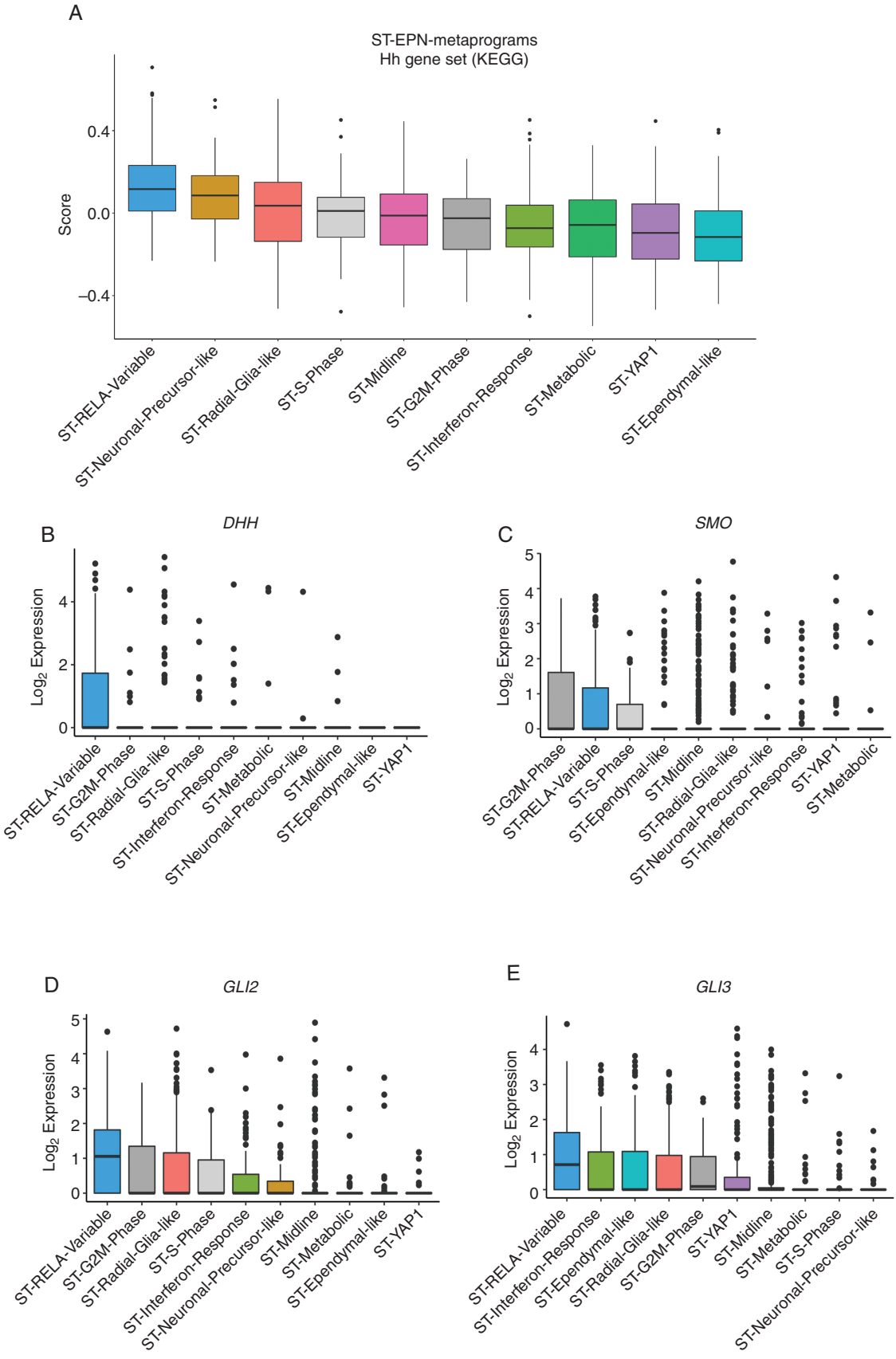

Fig. 2 Hh genes are enriched in undifferentiated and cycling ST-RELA cells. (A) Hh gene set score (KEGG_Hh pathway-hsa_04340) and (B–E) log-transformed expressions of Hh genes across the ST-EPNs metaprograms (GSE141460).[11]

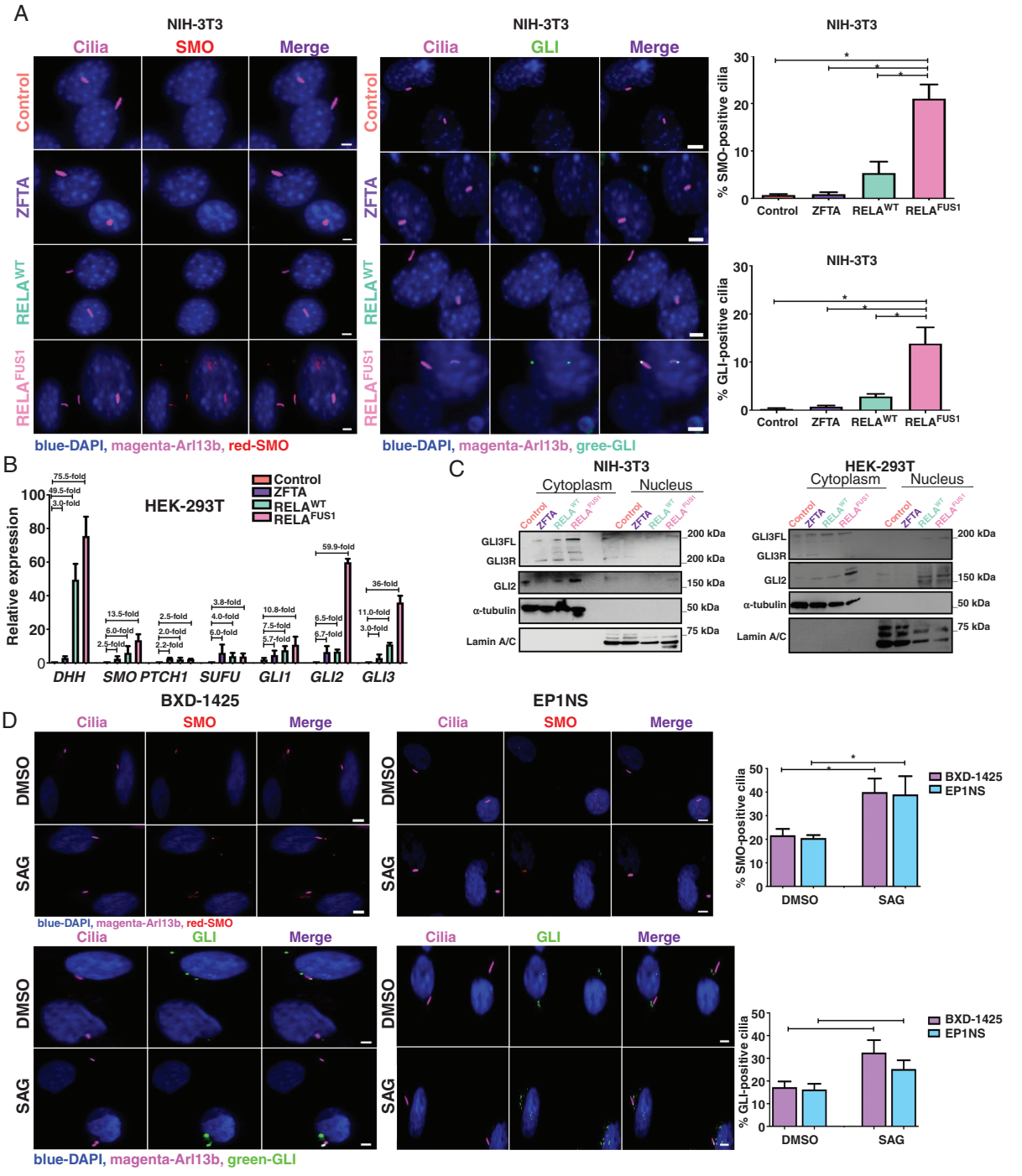

Fig. 3 Ligand-dependent Hh pathway activation induced by the RELA fusion. (A) Immunofluorescence staining and quantitative analysis of SMO and GLI-positive cilia in NIH-3T3 control, ZFTA, RELA^{WT}, or RELA^{FUS1} cells (scale bar = 1 μm). *$P < .05$, one-way ANOVA followed by Bonferroni test. (B) Hh gene expression in HEK-293T control, ZFTA, RELA^{WT}, or RELA^{FUS1} cells. (C) GLI2/3 protein expression in cytoplasmic and nuclear extracts of HEK-293T and NIH-3T3 control, ZFTA, RELA^{WT}, or RELA^{FUS1} cells. α-Tubulin and Lamin A/C were used as cytoplasmic and nuclear loading control, respectively. (D) Immunofluorescence staining and quantitative analysis of SMO and GLI-positive cilia after treatment with the SMO agonist, SAG (1 μM) (scale bar = 1 μm). *$P < .05$, Student's *t* test.

cells resulted in DHH release, paralleling the release of SHH from MEFs (Supplementary Figure 4A), a well-established system for studying Hh ligand release.[29] Lastly, we asked whether DHH secreted by BXD-1425 cells is active in Hh signaling. Treatment of NIH-3T3 cells with BXD-1425-conditioned media (CM) activated the Hh pathway, as measured by SMO and GLI recruitment to primary cilia (Supplementary Figure 4B). We also asked whether the

Hh pathway is active in ST-RELA cells. After confirming that primary cilia are present in BXD-1425 and EP1NS cells (Supplementary Figure 4C), we found that both cell lines show significant constitutive ciliary recruitment of SMO and GLI, which could be further increased by treatment with the SMO agonist, SAG (Figure 3D). In contrast, recruitment of SMO and GLI to cilia in MEFs was strictly dependent on SAG treatment (Supplementary Figure 4D). These results strongly support the idea of autocrine, DHH-dependent activation of Hh signaling in ST-RELA EPN-derived cell lines.

Hh Signaling Is a Primary Cilia-Dependent Therapeutic Vulnerability in ST-RELA Tumors

Given that we observed ligand-dependent Hh pathway activation in ST-RELA tumors, we next investigated the effect of Hh blockade by Sonidegib, a potent small molecule SMO antagonist under clinical evaluation for CNS tumors.[36,37] We found that Sonidegib reduces proliferation of BXD-1425 cells with IC_{50} = 32 µM, and of EP1NS cells with IC_{50} = 16 µM (Figure 4A); this anti-proliferative effect was accompanied by G2/M arrest (Supplementary Figure 5A). Furthermore, colony formation was strongly impaired by Sonidegib (Figure 4B), while cell death was enhanced (Figure 4C) for both cell lines. Consistent with the pro-apoptotic effect, Sonidegib treatment increased levels of p53 and BAX while reducing expression of the anti-apoptotic protein BCL-2 (Figure 4D). We next investigated the specificity of the Sonidegib effect on ST-RELA cells compared to other EPN subgroups. Interestingly, Sonidegib did not reduce proliferation in a PF-A cell line, MAF928[26] (Supplementary Figure 5B). Our results thus show that Hh signaling selectively regulates cell proliferation and apoptosis in ST-RELA in vitro models, suggesting a promising therapeutic vulnerability for this subgroup.

To test whether Hh inhibition is a valid therapeutic strategy for ST-RELA tumors, we next knocked out SMO and GLI2 in BXD-1425 cells by CRISPR/Cas9 (Supplementary Figure 5C). Consistent with the results of Sonidegib treatment, SMO- and GLI2-KO cells showed significant reduction in proliferation and G2/M cell cycle arrest compared to wild-type control cells (Supplementary Figure 5D and E). Interestingly, SMO-KO cells showed a reduction in proliferation of around 60%, compared to GLI2-KO cells which showed 35% reduction. This discrepancy is probably because we found a positive turnover of GLI3FL expression and reduction of GLI3R in GLI2-KO cells (Supplementary Figure 5C–E). These data further support testing of SMO inhibitors to impair the proliferation of ST-RELA tumors.

Despite the anti-proliferative and pro-apoptotic activity of Sonidegib, the observed IC_{50} values were not within a reasonable range for clinical application.[38,39] To address this limitation, we explored the underlying mechanisms controlling the response of ST-RELA cells to Sonidegib. It is well known that responsiveness to Sonidegib relies on the presence of primary cilia, which are required both for Hh activation by ligand and for proteolytic processing of GLI2 and 3 into the repressor forms in the unstimulated state of the Hh pathway[18,40] (Figure 4E). In Hh pathway-dependent cancer cells, loss of cilia abolishes susceptibility to SMO inhibitors, while maintaining a "persister" state dependent on continued activation of downstream Hh effectors.[40] This paradoxical effect is thought to be mediated by reduced formation of GLI2/3R upon cilia loss, leading to an increase in the FL, activating GLI2/3 species[18,40] (Figure 4F). Thus, we investigated the effect of Sonidegib on primary cilia and on the expression of upstream (DHH) and downstream (GLI) Hh pathway components.

Interestingly, substantial primary cilia loss was observed in BXD-1425 and EP1NS cells upon Sonidegib treatment (Figure 4G), accompanied by decreased expression of DHH and GLI1 (Supplementary Figure 5F). In contrast, Sonidegib had no effect on cilia in MEFs (Supplementary Figure 5G). These findings suggest that cilia loss is a ST-RELA-specific escape mechanism that reduces susceptibility to SMO inhibitors. Accordingly, loss of cilia was accompanied by increased levels of GLI2/3FL and concomitant reduction of GLI3R (Figure 4H). Since GLI3R formation requires primary cilia,[18,19] we hypothesized that cilia loss impairs GLI3FL processing to GLI3R in ST-RELA cells. Such a mechanism would drastically reduce responsiveness to upstream Hh pathway inhibition by Sonidegib, while also leading to downstream Hh pathway activation. To examine this hypothesis, we generated BXD-1425 cells without primary cilia (Supplementary Figure 5H), by knocking out *IFT88*[17] using CRISPR/Cas9. Interestingly, IFT88-KO cells showed increased proliferation compared to wild-type control cells (Supplementary Figure 5I). Moreover, Sonidegib showed no effects on the proliferation rate of IFT88-KO cells, in contrast to control cells (Supplementary Figure 5J). Consistent with cilia loss, IFT88-KO cells had elevated levels of GLI2/3FL, and reduced levels of GLI3R (Supplementary Figure 5K). These results indicate that Sonidegib-induced cilia loss in ST-RELA cells mediates a compensatory feed-forward mechanism of therapeutic escape, reducing susceptibility to SMO inhibition while increasing downstream Hh signaling.

Alisertib Rescues Ciliogenesis and Responsiveness to Sonidegib In Vitro But Shows No Effect In Vivo

We next sought to identify strategies to reverse loss of cilia and rescue Sonidegib responsiveness in ST-RELA cells. A key protein promoting cilia disassembly is the AURKA, which localizes to the ciliary base[41] (Figure 5A). Using qRT-PCR, microarray, and scRNA-seq data,[2,11] we found that *AURKA* is overexpressed selectively in ST-RELA tumors, mainly in cell cycle-active ST-G2M-Phase and ST-S-Phase subpopulations, and in ST-RELA cell lines compared to other EPN subgroups; this expression pattern supports the idea of combined Hh and AURKA inhibition, to specifically target stem-like ST-RELA compartments (Supplementary Figure 6A and B). Interestingly, SMO inhibition had no effect on AURKA expression, or on its activating phosphorylation (pAURKA) at the ciliary basal body[22,41] (Figure 5B and C, Supplementary Figure 6C), suggesting that AURKA is active even under Sonidegib treatment and may promote cilia disassembly in ST-RELA models. AURKA inhibition by Alisertib, a potent inhibitor currently evaluated clinically in adult anaplastic EPNs,[42] reduced AURKA expression,

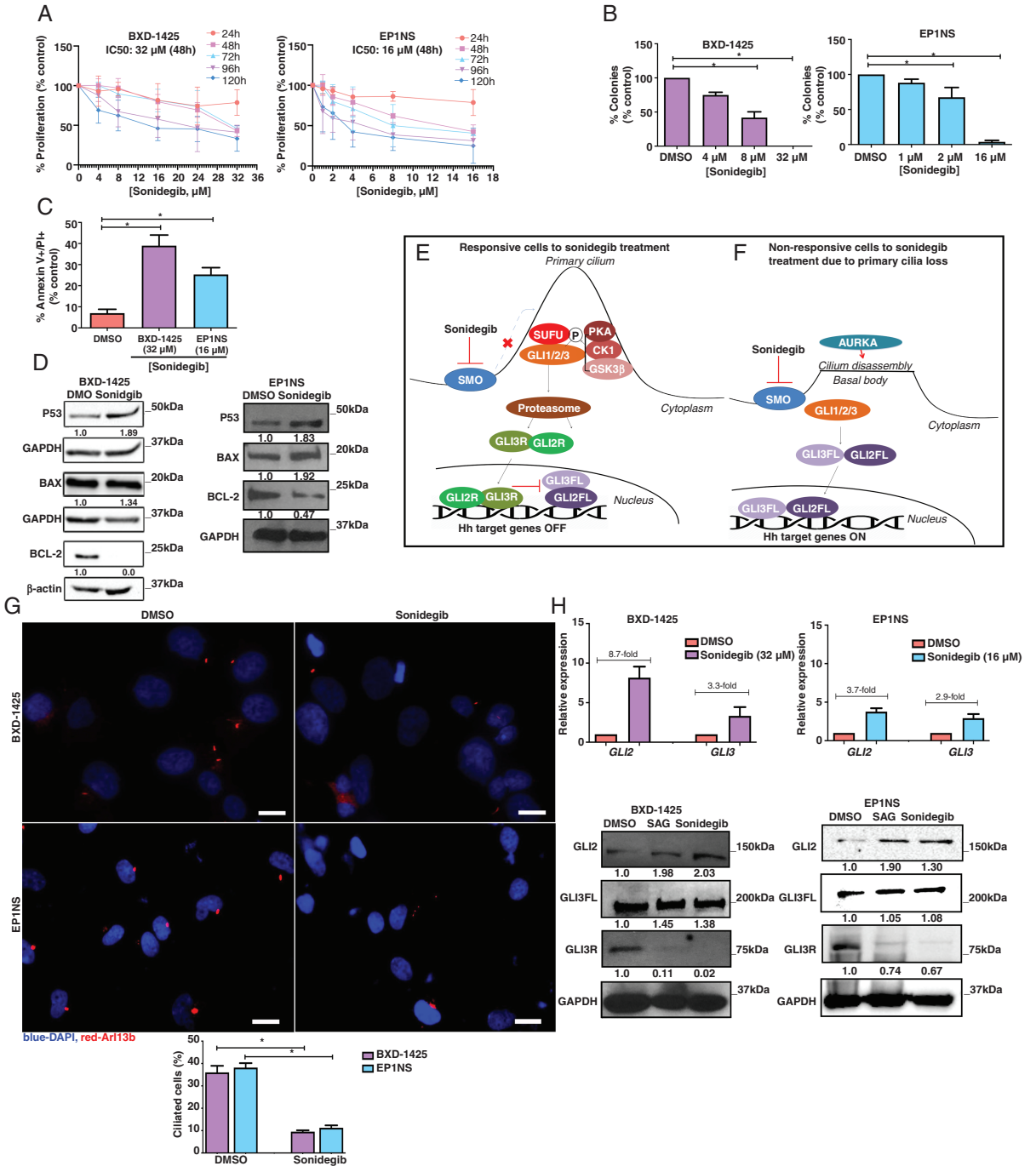

Fig. 4 Effect of Sonidegib on ST-RELA cells. (A) Cell proliferation after exposure (24-120 h) to Sonidegib, as measured by CCK-8. IC_{50} values were obtained with CalcuSyn after 48-hour treatment. $^*P < .05$, one-way ANOVA followed by Bonferroni test. (B) Colony formation, (C) Annexin V/propidium iodide (PI)-positive cells, and (D) P53, BAX, and BCL-2 protein expression after treatment for 48 h with Sonidegib, at IC_{50}/cell line. $^*P < .05$, one-way ANOVA followed by Bonferroni test. (E) Schematic of the effect of Sonidegib on the Hh pathway. Sonidegib binds SMO and blocks its activation and translocation to primary cilia. Consequently, the latent SUFU-GLI complex is maintained in the cytoplasm, thereby inhibiting the nuclear translocation of GLI proteins. Additionally, protein kinase A (PKA), glycogen synthase kinase 3β (GSK-3β), and casein kinase 1 (CK1) promote formation of the GLI repressor (GLI2/3R), which translocates to the nucleus and inhibits Hh signaling. (F) In the absence of cilia, Sonidegib shows poor effectiveness/activity, and the GLI proteolytic process is compromised. Thus, the active form of GLI (GLI2/3FL) builds up and activates the transcription of Hh target genes. (G) Immunofluorescence staining and quantitative analysis of primary cilia (Arl13b, red) and (H) GLI2/3 gene and protein expression after 48 hours of Sonidegib at IC_{50}/cell line (scale bar = 10 µm). $^*P < .05$, Student's *t* test. GAPDH or β-actin were used as loading controls. Quantification of proteins was performed using ImageJ software.

and phosphorylation (Figure 5B and C, Supplementary Figure 6C). Dramatically, Alisertib reversed Sonidegib-induced cilia loss in BXD-1425 and EP1NS cells (Figure 5D). Combining Alisertib and Sonidegib strongly reduced total and phosphorylated AURKA levels and increased the number of ciliated cells (Figure 5B and D, Supplementary Figure 6C), while also promoting formation of GLI3R at the expense of the GLI2/3FL precursor (Figure 5E).

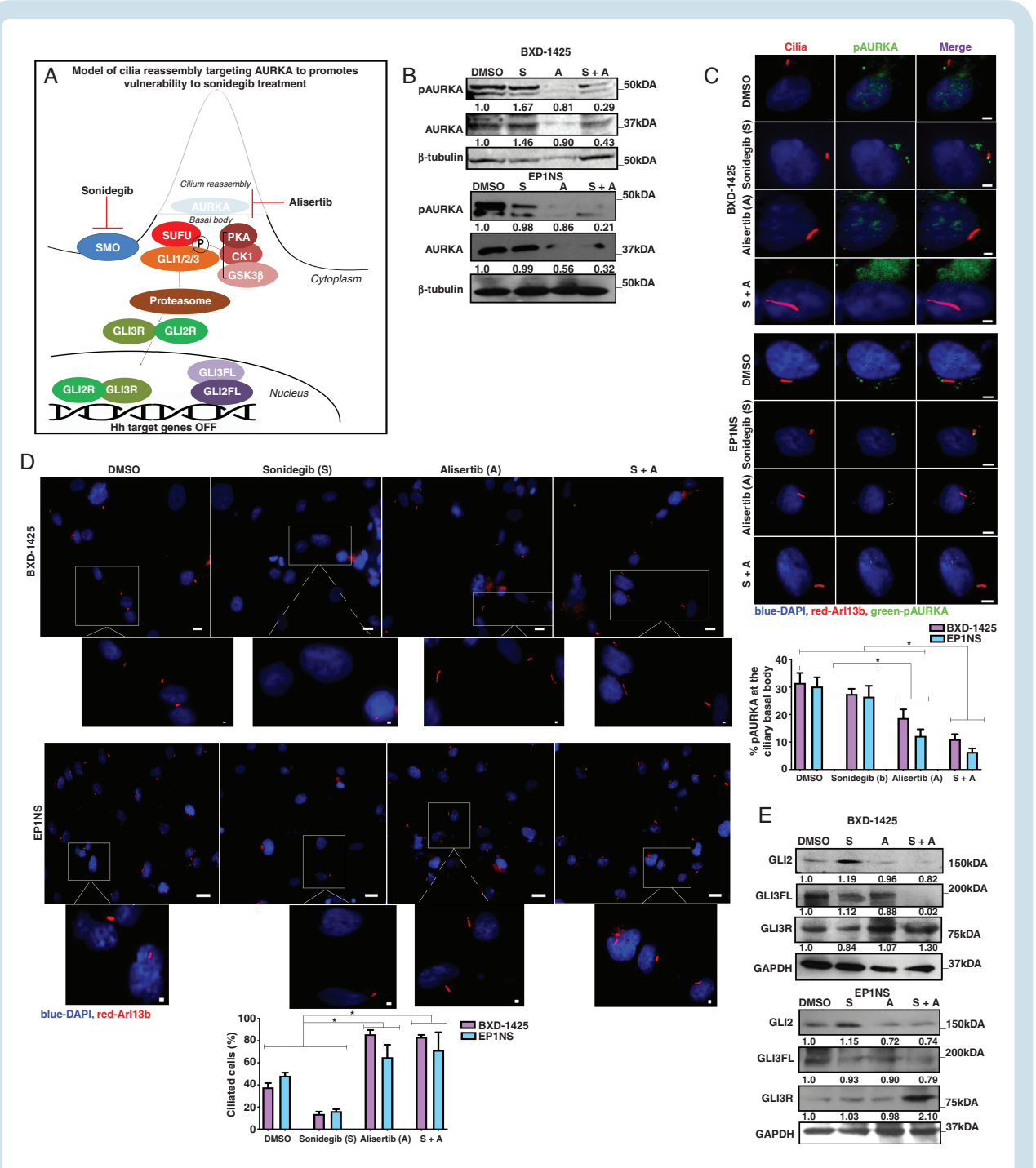

Fig. 5 Alisertib shifts ST-RELA cells into a "ciliated phenotype," which permits the action of Sonidegib. (A) AURKA inhibition by Alisertib promotes reassembly of primary cilia, thus rescuing GLI3 processing to GLI3R. (B) Expression of AURKA protein and its phosphorylation (pAURKA) and (C) immunofluorescence staining and quantitative analysis of pAURKA at the basal body of primary cilia, following a 48-hour treatment with the indicated drugs alone (IC_{50}/cell line), or in combination (scale bar = 1 μm). *$P < .05$, one-way ANOVA followed by Bonferroni test. (D) Immunofluorescence staining and quantitative analysis of primary cilia (Arl13b, red) and (E) GLI2/3 protein expression after 48-hour treatment with indicated drugs alone (IC_{50}/cell line) or in combination (scale bar = 10 and 1 μm). *$P < .05$, one-way ANOVA followed by Bonferroni test. GAPDH or β-tubulin were used as loading controls. Quantification of proteins was performed using ImageJ software.

We further sought to determine whether AURKA inhibition influences the response to Sonidegib. The combination of Sonidegib and Alisertib led to drastic reduction of SMO-positive cilia and expression of *DHH*, *GLI1*, *GLI2*, and *GLI3* in BXD-1425 and EP1NS cells, compared to monotherapy (Figure 6A and B). Moreover, Sonidegib and Alisertib showed strong synergy in reducing proliferation and colony formation and increasing G2/M-phase arrest and cell death (Figure 6C and D, Supplementary Figure 6D–G); importantly, these effects occurred at lower, clinically relevant doses compared to single-drug treatments.

Finally, we assayed the effect of the drug combination in an IC-1425EPN xenograft ST-RELA model.[24] To this end, mice were treated on a daily basis for 20 days with 80 mg/kg of Sonidegib and 30 mg/kg of Alisertib, alone or in combination, after the luciferase signal reached 10^7 p/seconds/cm^2/sr. These treatments did not show a survival benefit or tumor shrinkage in this in vivo model (Figure 6E, Supplementary Figure 7A). To determine if the administered drugs were present within xenografts, we assayed molecular markers for both drugs. While cilia loss was reproducibly observed in most cells, indicating that Sonidegib is reaching tumor cells (Figure 6F), no differences in total or phosphorylated AURKA were observed (Supplementary Figure 7B), suggesting poor penetration by Alisertib, which can explain the lack of cilia rescue. This effect jeopardizes the effect of Sonidegib on Hh signaling, as we found SMO-positive cilia in the remaining ciliated cells, as well as predominant expression of nuclear GLI2 in Sonidegib-treated tumors (Figure 6F, Supplementary Figure 7C). Together, these data reinforce the critical need of cilia reassembly for an effective response to Hh pathway inhibition in vivo.

Discussion

The poor outcome of the standard care of therapy for ST-RELA patients (surgical resection and/or radiotherapy)[2–4] and the lack of alternative therapeutic options represent an urgent challenge.[3] The Hh pathway is a key regulator of CNS development and has been suggested as a promising target in brain cancers.[13,38] Although aberrant Hh signaling may be important in the pathogenesis of pediatric EPNs,[7,12,16,43] its role in ST-RELA tumors has not been explored. Here, we demonstrate that Hh signaling has a key role in regulating cell proliferation and aggressiveness of ST-RELA tumors. We discover that ST-RELA cells subjected to Hh pathway blockade at the level of SMO become refractory to the SMO inhibitor by loss of primary cilia. Strikingly, cilia assembly can be restored in these cells by pharmacological inhibition of AURKA, which also rescues the effect of SMO inhibition. Thus, our present work suggests the value of combining AURKA and SMO inhibitors, as a novel therapeutic approach in ST-RELA tumors.

In this study, we cross-validated in three distinct cohorts that ST-RELA tumors bear a specific Hh signature compared to other EPN subgroups, including key Hh genes *DHH*, *SMO*, *GLI2*, and *GLI3*. Furthermore, a scRNA-seq dataset revealed that Hh genes are selectively enriched in ST-RELA stem cell compartments conferring poor patient outcome.[11] Therefore, Hh inhibition is an attractive approach to specifically target those subpopulations that contribute the most to the therapy refractoriness of this tumor type.[11]

Expression of Hh pathway components has been proven as predictive for responsiveness to SMO inhibitors in other brain tumors.[36,37] However, these tumors bear Hh driver mutations, which leads to constitutive Hh pathway activation even in the absence of Hh ligands.[36,37] Given that Hh mutations are not found in ST-RELA tumors,[2,33] we hypothesized that Hh signaling in this case is ligand-dependent. Accordingly, we found that the oncogenic RELA fusion induces DHH expression, resulting in Hh pathway activation, as indicated by translocation of SMO and GLI to primary cilia, and of GLI2/3FL to the nucleus. In line with this finding, we found that ST-RELA cells secrete functional DHH ligand, consistent with the Hh signature present in tumor samples. Furthermore, the SMO inhibitor, Sonidegib, and loss-of-function experiments against SMO and GLI2 revealed SMO inhibition as a therapeutic vulnerability in in vitro ST-RELA models, corroborating the well-known role of Hh signaling in several CNS tumors.[18–20]

Despite the anti-proliferative and pro-apoptotic activity of Sonidegib on cultured ST-RELA cells, the IC_{50} was not within the acceptable range for clinical applications.[38,39] Considering that primary cilia are critical for SMO inhibition,[18] we found that Sonidegib treatment leads to significant cilia loss, which is followed by reduced GLI3R expression and increased GLI2/3FL. Studies in other CNS tumors (medulloblastoma, glioblastoma, and astrocytoma) show that primary cilia are necessary for proteolytic processing of FL GLI2/3 into their repressor forms.[18,19,40] Based on this, we hypothesized that cilia loss in ST-RELA tumors allows escape from SMO inhibition while also activating downstream Hh signaling at the level of GLI proteins.

Several authors proposed strategies to promote vulnerability to SMO inhibitors, by either treating with GLI inhibitors or targeting proteins that promote cilia disassembly.[17,22] Targeting a GLI protein can induce positive regulatory activity of other GLI members or can counteract the inhibitor GLI3R.[44] Instead, AURKA inhibitors, such as Alisertib can block ciliary disassembly and thus maintain upstream Hh signaling.[22,41] We found that *AURKA* is highly expressed in ST-RELA tumors, mainly in cell cycle-active cell subpopulations, suggesting a potential role in cilia loss. In line with this idea, AURKA inhibition by Alisertib, alone or in combination with Sonidegib, caused strong cilia stabilization, increased GLI3R and decreased GLI2/3FL levels, and promoted cell death in ST-RELA cell models, at clinically relevant drug concentrations.

Consistent with our results in cell lines, the in vivo data show that Sonidegib promotes cilia loss as an escape mechanism, allowing cells to circumvent Hh inhibition. However, Alisertib did not inhibit AURKA in vivo, perhaps because it did not reach the xenografts. Although previous reports showed high bioavailability of Alisertib in brain tumors,[42] a recent study demonstrated that penetration of Alisertib within CNS is limited by blood-brain barrier drug efflux pumps.[45] These observations might explain the lack of cilia rescue by Alisertib in vivo and the lack of synergy with Sonidegib that occurs in cultured cells. Thus, primary cilia reassembly is critical for the response to Hh inhibitors in ST-RELA tumors. Improved delivery methods for AURKA inhibitors, such as intrathecal delivery,[46] will be key to potentiating the therapeutic vulnerability of ST-RELA tumors.

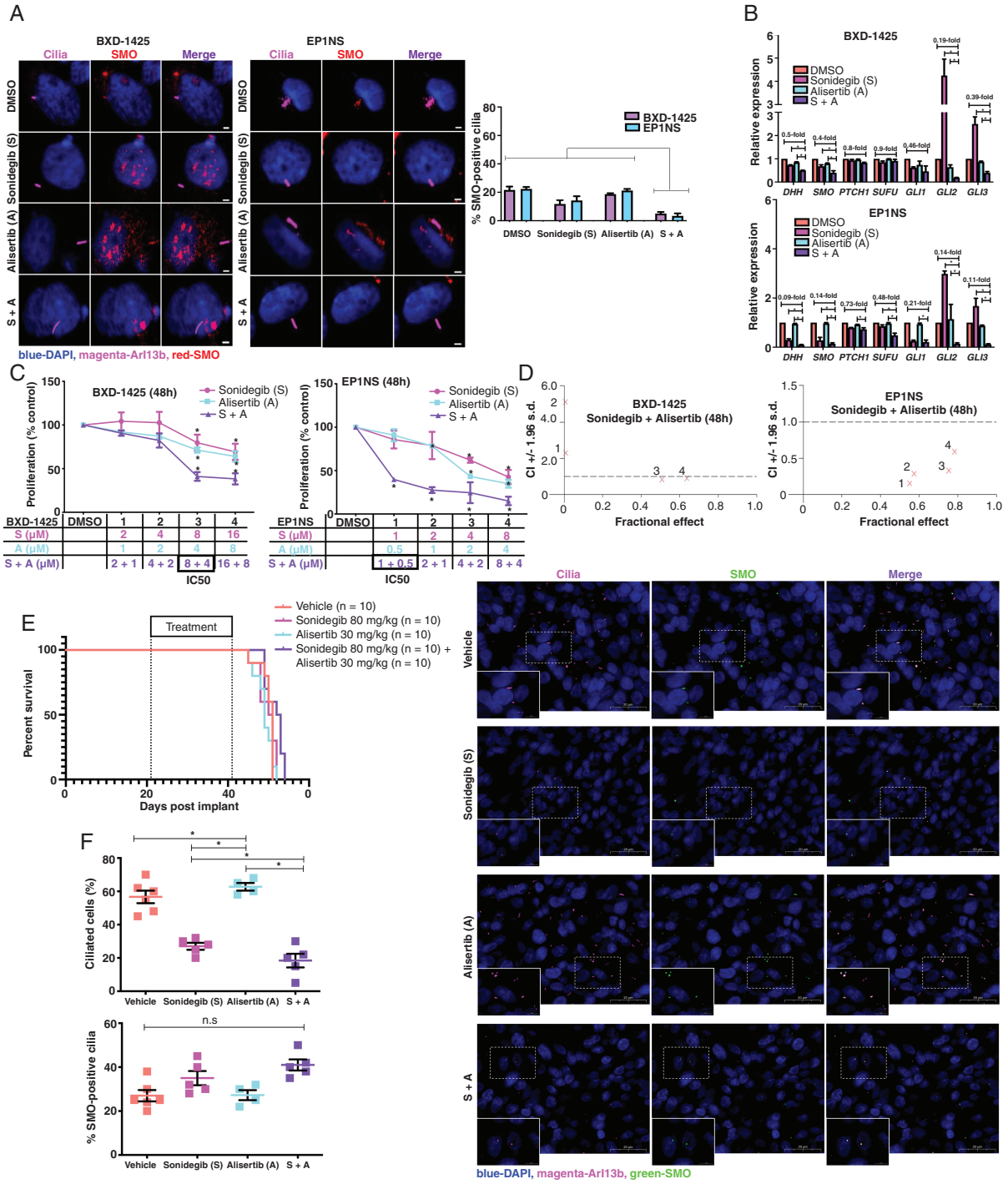

Fig. 6 Alisertib reduces cellular proliferation and increases cell death in cell culture, but not in vivo. (A) Immunofluorescence staining and quantitative analysis of SMO-positive cilia and (B) Hh gene expression after 48-hour treatment with the indicated drugs alone (IC_{50}/cell line) or in combination (scale bar = 1 µm). *P < .05, one-way ANOVA followed by Bonferroni test. (C) Cell proliferation following a 48-hour treatment with drugs alone or in combination, as measured by CCK-8. (D) Combination index (CI) values for the drug combination in (C). The dashed line at CI = 1 indicates an additive effect; CIs above and below 1 indicate antagonism and synergism, respectively. Crosses (x) represent the CIs of actual data points determined using CalcuSyn. *P < .05, one-way ANOVA followed by Bonferroni test. (E) Survival curves of mice with orthotopic IC-1425EPN xenografts treated with drugs alone or in combination. Drug concentration and number of animals per group are indicated (mg/kg; n). (F) Immunofluorescence staining and quantitative analysis of primary cilia (Arl13b, magenta) and SMO-positive cilia in IC-1425EPN xenografts, after oral treatment with drugs alone or in combination (80 mg/kg of Sonidegib or/and 30 mg/kg of Alisertib 5×/week; p.o.) (scale bar = 20 µm). *P < .05, one-way ANOVA followed by Bonferroni test.

In summary, our study shows that Hh pathway components are selectively overexpressed in ST-RELA tumors, being induced by the RELA fusion. We find that loss of primary cilia is the mechanism by which ST-RELA cells become resistant to SMO inhibition by Sonidegib. We demonstrate that rescuing cilia assembly by the AURKA inhibitor, Alisertib, greatly enhances vulnerability to Hh inhibition; this explains the synergistic effect of Alisertib and Sonidegib on ST-RELA cells. Our in vivo data confirm that Sonidegib promotes cilia loss, and that Hh signaling is a primary cilia-dependent therapeutic vulnerability in ST-RELA tumors. However, ineffective AURKA inhibition in tumors precluded cilia reassembly and thus limited the benefit of the Sonidegib-Alisertib combination. These findings support the need for further studies on primary cilia rescue, to restore vulnerability to Hh inhibition and specifically target highly aggressive ST-RELA tumor cell niches.

Supplementary Material

Supplementary material is available at *Neuro-Oncology* online.

Keywords

Alisertib | Hedgehog pathway | Primary cilia | Sonidegib | ST-RELA ependymoma

Funding

This study was supported by the São Paulo Research Foundation (FAPESP) [2014/20341-0/Brazil, 2016/19820-6/Brazil, and 2018/18842-1/Brazil to T.A.M.]; Erwin Schrödinger Fellowship of the Austrian Science Fund [J-4311 to B.E.] Pirate Ship Foundation (no specific number required) to R.E. NIH grants R01 GM122920 and R01 GM135262 to A.S. Fundação de Amparo ao Ensino, Pesquisa e Assistência - FMRP-USP (FAEPA) (no specific number required) to C.A.S.

Acknowledgments

We thank Dr Xiao-Nan Li, Northwestern University, for providing the BXD-1425EPN cell line and IC-1425EPN PDX model, Dr Till Milde, Hopp Children's Cancer Center (KiTZ) and German Cancer Research Center (DKFZ), for providing the DKFZ-EP1NS cell line, Dr Nicholas K Foreman, University of Colorado, for providing the MAF928 cell line, Dr. Richard Gilbertson, Cancer Research UK Cambridge Institute, for providing the plasmids, and the Bioresources team of Telethon Kids Institute for the care of our animals.

Conflict of interest statement. The authors declare no conflicts of interest.

Authorship statement. T.A.M. performed all experiments. G.A.V.C., G.R.S., M.A., K.R.S., C.L.Y., B.C., and M.K. performed experiments. T.A.M., L.F.N., B.E., L.J., and J.G. performed in silico analysis. F.P.S., S.K.N.M., S.M.O., J.A.Y., R.E., and M.G.F. provided reagents and data. R.G.P.Q., C.A.S., K.S.B., A.S., L.G.T., and E.T.V. provided consultation. T.A.M., A.S., and E.T.V. wrote the manuscript, with input from all the authors.

References

1. Louis DN, Perry A, Wesseling P, et al. The 2021 WHO classification of tumors of the central nervous system: a summary. *Neuro Oncol.* 2021;23(8):1231–1251.
2. Pajtler KW, Witt H, Sill M, et al. Molecular classification of ependymal tumors across all CNS compartments, histopathological grades, and age groups. *Cancer Cell.* 2015;27(5):728–743.
3. Pajtler KW, Mack SC, Ramaswamy V, et al. The current consensus on the clinical management of intracranial ependymoma and its distinct molecular variants. *Acta Neuropathol.* 2017;133(1):5–12.
4. Pajtler KW, Wen J, Sill M, et al. Molecular heterogeneity and CXorf67 alterations in posterior fossa group A (PFA) ependymomas. *Acta Neuropathol.* 2018;136(2):211–226.
5. Cavalli FMG, Hübner J-M, Sharma T, et al. Heterogeneity within the PF-EPN-B ependymoma subgroup. *Acta Neuropathol.* 2018;136(2):227–237.
6. Arabzade A, Zhao Y, Varadharajan S, et al. ZFTA–RELA dictates oncogenic transcriptional programs to drive aggressive supratentorial ependymoma. *Cancer Discov.* 2021;11(9):2200–2215.
7. Kupp R, Ruff L, Terranova S, et al. ZFTA translocations constitute ependymoma chromatin remodeling and transcription factors. *Cancer Discov.* 2021;11(9):2216–2229.
8. Fukuoka K, Kanemura Y, Shofuda T, et al. Significance of molecular classification of ependymomas: C11orf95-RELA fusion-negative supratentorial ependymomas are a heterogeneous group of tumors. *Acta Neuropathol Commun.* 2018;6(1):134.
9. de Almeida Magalhães T, Cruzeiro GAV, de Sousa GR, et al. Notch pathway in ependymoma RELA-fused subgroup: upregulation and association with cancer stem cells markers expression. *Cancer Gene Ther.* 2020;27(6):509–512.
10. Ozawa T, Arora S, Szulzewsky F, et al. A de novo mouse model of C11orf95-RELA fusion-driven ependymoma identifies driver functions in addition to NF-κB. *Cell Rep.* 2018;23(13):3787–3797.
11. Gojo J, Englinger B, Jiang L, et al. Single-cell RNA-Seq reveals cellular hierarchies and impaired developmental trajectories in pediatric ependymoma. *Cancer Cell.* 2020;38(1):44–59.e9.
12. de Bont JM, Packer RJ, Michiels EM, den Boer ML, Pieters R. Biological background of pediatric medulloblastoma and ependymoma: a review from a translational research perspective. *Neuro Oncol.* 2008;10(6):1040–1060.
13. Fattahi S, Pilehchian Langroudi M, Akhavan-Niaki H. Hedgehog signaling pathway: epigenetic regulation and role in disease and cancer development. *J Cell Physiol.* 2018;233(8):5726–5735.
14. Taylor MD, Poppleton H, Fuller C, et al. Radial glia cells are candidate stem cells of ependymoma. *Cancer Cell.* 2005;8(4):323–335.
15. Petrov K, Wierbowski BM, Liu J, Salic A. Distinct cation gradients power cholesterol transport at different key points in the hedgehog signaling pathway. *Dev Cell.* 2020;55(3):314–327.e7.

16. Zhong S, Yan Q, Ge J, Dou G, Zhao G. Identification of driver genes and key pathways of ependymoma. *Turk Neurosurg.* 2018; 21876-17.5 [Epub ahead of print].
17. Liu H, Kiseleva AA, Golemis EA. Ciliary signalling in cancer. *Nat Rev Cancer.* 2018;18(8):511–524.
18. Goranci-Buzhala G, Gabriel E, Mariappan A, Gopalakrishnan J. Losers of primary cilia gain the benefit of survival. *Cancer Discov.* 2017;7(12):1374–1375.
19. Peer E, Tesanovic S, Aberger F. Next-generation hedgehog/GLI pathway inhibitors for cancer therapy. *Cancers (Basel).* 2019;11(4):538.
20. Wong SY, Seol AD, So P-L, et al. Primary cilia can both mediate and suppress Hedgehog pathway-dependent tumorigenesis. *Nat Med.* 2009;15(9):1055–1061.
21. Dong X, Wang C, Chen Z, Zhao W. Overcoming the resistance mechanisms of Smoothened inhibitors. *Drug Discov Today.* 2018;23(3):704–710.
22. Nikonova AS, Astsaturov I, Serebriiskii IG, Dunbrack RL, Golemis EA. Aurora A kinase (AURKA) in normal and pathological cell division. *Cell Mol Life Sci.* 2013;70(4):661–687.
23. de Sousa GR, Lira RCP, de Almeida Magalhães T, et al. A coordinated approach for the assessment of molecular subgroups in pediatric ependymomas using low-cost methods. *J Mol Med.* 2021;99(8):1101–1113.
24. Yu L, Baxter PA, Voicu H, et al. A clinically relevant orthotopic xenograft model of ependymoma that maintains the genomic signature of the primary tumor and preserves cancer stem cells in vivo. *Neuro Oncol.* 2010;12(6):580–594.
25. Milde T, Kleber S, Korshunov A, et al. A novel human high-risk ependymoma stem cell model reveals the differentiation-inducing potential of the histone deacetylase inhibitor Vorinostat. *Acta Neuropathol.* 2011;122(5):637–650.
26. Amani V, Donson AM, Lummus SC, et al. Characterization of 2 novel ependymoma cell lines with chromosome 1q gain derived from posterior fossa tumors of childhood. *J Neuropathol Exp Neurol.* 2017;76(7):595–604.
27. Parker M, Mohankumar KM, Punchihewa C, et al. C11orf95–RELA fusions drive oncogenic NF-κB signalling in ependymoma. *Nature.* 2014;506(7489):451–455.
28. Ran FA, Hsu PD, Wright J, et al. Genome engineering using the CRISPR-Cas9 system. *Nat Protoc.* 2013;8(11):2281–2308.
29. Wierbowski BM, Petrov K, Aravena L, et al. Hedgehog pathway activation requires coreceptor-catalyzed, lipid-dependent relay of the sonic hedgehog ligand. *Dev Cell.* 2020;55(4):450–467.e8.
30. Yao CD, Haensel D, Gaddam S, et al. AP-1 and TGFß cooperativity drives non-canonical Hedgehog signaling in resistant basal cell carcinoma. *Nat Commun.* 2020;11(1):5079.
31. Xin Y, Ning S, Zhang L, Cui M. CDC27 facilitates gastric cancer cell proliferation, invasion and metastasis via twist-induced epithelial-mesenchymal transition. *Cell Physiol Biochem.* 2018;50(2):501–511.
32. Hovestadt V, Smith KS, Bihannic L, et al. Resolving medulloblastoma cellular architecture by single-cell genomics. *Nature.* 2019;572(7767):74–79.
33. Malgulwar PB, Nambirajan A, Pathak P, et al. *C11orf95-RELA* fusions and upregulated NF-KB signalling characterise a subset of aggressive supratentorial ependymomas that express L1CAM and nestin. *J Neurooncol.* 2018;138(1):29–39.
34. Huang P, Nedelcu D, Watanabe M, et al. Cellular cholesterol directly activates smoothened in hedgehog signaling. *Cell.* 2016;166(5):1176–1187.e14.
35. Cai K, Na W, Guo M, et al. Targeting the cross-talk between the hedgehog and NF-κB signaling pathways in multiple myeloma. *Leuk Lymphoma.* 2019;60(3):772–781.
36. Kieran MW, Chisholm J, Casanova M, et al. Phase I study of oral sonidegib (LDE225) in pediatric brain and solid tumors and a phase II study in children and adults with relapsed medulloblastoma. *Neuro Oncol.* 2017;19(11):1542–1552.
37. Kool M, Jones DTW, Jäger N, et al. Genome sequencing of SHH medulloblastoma predicts genotype-related response to smoothened inhibition. *Cancer Cell.* 2014;25(3):393–405.
38. Fu J, Rodova M, Nanta R, et al. NPV-LDE-225 (Erismodegib) inhibits epithelial mesenchymal transition and self-renewal of glioblastoma initiating cells by regulating miR-21, miR-128, and miR-200. *Neuro Oncol.* 2013;15(6):691–706.
39. Markant SL, Esparza LA, Sun J, et al. Targeting sonic hedgehog-associated medulloblastoma through inhibition of aurora and polo-like kinases. *Cancer Res.* 2013;73(20):6310–6322.
40. Zhao X, Pak E, Ornell KJ, et al. A transposon screen identifies loss of primary cilia as a mechanism of resistance to SMO inhibitors. *Cancer Discov.* 2017;7(12):1436–1449.
41. Kiseleva AA, Korobeynikov VA, Nikonova AS, et al. Unexpected activities in regulating ciliation contribute to off-target effects of targeted drugs. *Clin Cancer Res.* 2019;25(13):4179–4193.
42. Song A, Andrews DW, Werner-Wasik M, et al. Phase I trial of alisertib with concurrent fractionated stereotactic re-irradiation for recurrent high grade gliomas. *Radiother Oncol.* 2019;132:135–141.
43. Zheng T, Ghasemi DR, Okonechnikov K, et al. Cross-species genomics reveals oncogenic dependencies in ZFTA/C11orf95 fusion-positive supratentorial ependymomas. *Cancer Discov.* 2020;11(9):2230–2247.
44. Infante P, Alfonsi R, Botta B, Mori M, Di Marcotullio L. Targeting GLI factors to inhibit the Hedgehog pathway. *Trends Pharmacol Sci.* 2015;36(8):547–558.
45. Power E, Oh J, Zhang L, Elmquist W, Daniels D. HGG-13. Brain distribution and clearance of alisertib is limited by PGP and BCRP efflux pumps and dependent upon delivery method. *Neuro Oncol.* 2021;23(Supplement_1):i20.
46. Shen Y, Ding Z, Ma S, et al. Targeting aurora kinase B alleviates spinal microgliosis and neuropathic pain in a rat model of peripheral nerve injury. *J Neurochem.* 2020;152(1):72–91.

Imvax®

NOW ENROLLING

Phase 2b study of IGV-001 in patients with newly diagnosed glioblastoma (NCT04485949)

OBJECTIVES

PRIMARY OBJECTIVE
Progression-free survival

SECONDARY OBJECTIVE
Overall survival

SAFETY OBJECTIVE
Safety and tolerability

CRITERIA

Key Inclusion Criteria

Patients who take part in the trial* must:

- Have newly diagnosed glioblastoma
- Be 18 to 70 years of age
- Have a KPS score ≥70 (unable to work but able to care for themselves overall)

Key Exclusion Criteria

Patients are not allowed to participate* in the trial if they have:

- A tumor that is on both sides of the brain
- Had previous surgery or anticancer treatment for glioblastoma
- Glioblastoma that came back
- Another cancer† while having glioblastoma or within the last 3 years that is not cured
- A weakened immune system (example: HIV, HBV, HCV) or an autoimmune disorder (example: Crohn's disease)
- Heart disease or history of heart issues

LEARN MORE
imvax.com/patients-families

LEARN MORE
clinicaltrials.gov/ct2/show/NCT04485949

*Additional criteria apply. Please refer to protocol 14379-201 for full inclusion and exclusion criteria. †Patients can participate if they had some skin cancers, superficial bladder cancer (cancer that was only on the surface of the lining of the bladder), or carcinoma in situ (cancer that had not spread) of the cervix or breast that had been cured.

HIV, human immunodeficiency virus; HBV, hepatitis B virus; HCV, hepatitis C virus; IGF-1R, insulin-like growth factor 1 receptor; KPS, Karnofsky Performance Scale; RT, radiotherapy; SOC, standard of care; TMZ, temozolomide.